ORGANIC CHEMISTRY

FRONTIERS

Accepted Manuscript

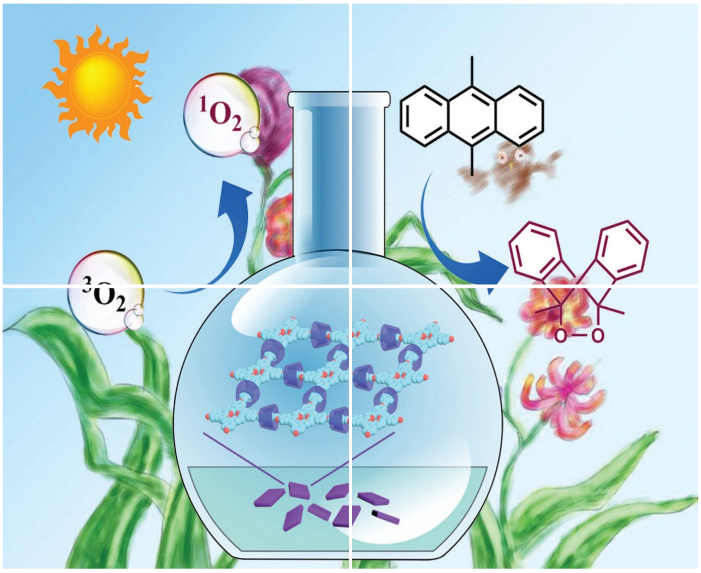

This article can be cited before page numbers have been issued, to do this please use: M. Gil, A. Maestro, P. Ortega, P. G. Jambrina and J. M. Andres, *Org. Chem. Front.*, 2022, DOI: 10.1039/D1QO01462E.

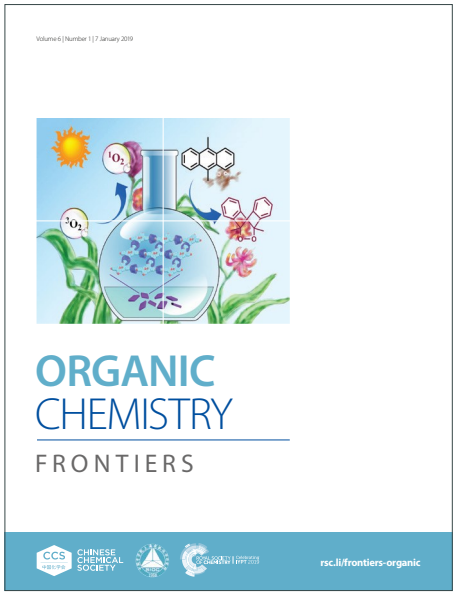

DOI: 10.1039/D1QO01462E

ARTICLE

NHC-Catalysed [3+2]-Asymmetric Annulation between Pyrazolin-4,5-diones and Enals: Synthesis of Novel Spirocyclic Pyrazolone γ-Butyrolactones and Computational Study of Mechanism and Stereoselectivity

Received 00th January 20xx,
Accepted 00th January 20xx

DOI: 10.1039/x0xx00000x

Marta Gil-Ordóñez,[a] Alicia Maestro,*[a] Pablo Ortega,[b] Pablo G. Jambrina,[b] José M. Andrés*[a]

Chiral pyrazolones with a spirocyclic centre at the C4-position are widely found in a large family of medically relevant compounds. In recent years, organocatalysis, particularly that performed with quiral *N*-heterocyclic carbenes (NHCs), has allowed the enantioselective synthesis of these spirocyclic compounds despite its inherent difficulty. In this work, we describe the fully diastereo- and highly enantioselective synthesis of novel spirocyclic pyrazolone γ-butyrolactones via NHC-catalysed [3+2] annulation reaction of enals and 1*H*-pyrazol-4,5-diones. To understand the catalytic mechanism and origin of stereoselectivity, electronic structure calculations were carried out. After considering various pathways, we concluded that stereoselectivity-determining step is the formation of the lactone that proceeds after addition of the NHC derived homoenolate to the electrophilic carbonyl group of pyrazolin-4,5-dione. Our calculations predict that the free energy barrier is lower for the (*RS*) product, which is also the main product experimentally obtained.

Introduction

A five-membered heterocycle with two adjacent nitrogen atoms such as the pyrazole ring stands out within the exclusive world of heterocyclic systems.[1] Not only does it play a prominent role in materials[2] and coordination chemistry,[3] its pyrazol-3-one derivatives also exhibit a broad spectrum of potent biological and pharmaceutical activities.[4] In particular, the asymmetric synthesis of pyrazolones with a quaternary spirocyclic centre at the C4 position has attracted the attention from synthetic chemists because spiropyrazolones combine their well-known biological properties with others provided by the rigidity of the skeleton present in spiro compounds (Figure 1).[5]

Over the past few years some organocatalytic strategies have been developed to access spiropyrazolones with a heteroatom incorporated in the chiral spirocentre.[6] Wang group has used quinine-derived thioureas and squaramides for the construction of spiro 4-aminopiropyrazolones from versatile 4-isothiocyanato pyrazolones.[7] There are also not many examples describing access to chiral spirocyclic pyrazolones bearing a 4-oxygen incorporated spirocentre. The diastereodivergent and enantioselective epoxidation of unsaturated pyrazolones developed by the Lattanzi group provide *trans*- or *cis*-spiropyrazolone epoxides using amine-thioureas as effective catalysts.[8] Likewise, the bifunctional squaramide-catalysed reaction of in-situ-generated *o*-quinone methides with pyrazolin-5-ones and 4-halo pyrazolones provides easy access to chiral spiro-benzofuran pyrazolones.[9]

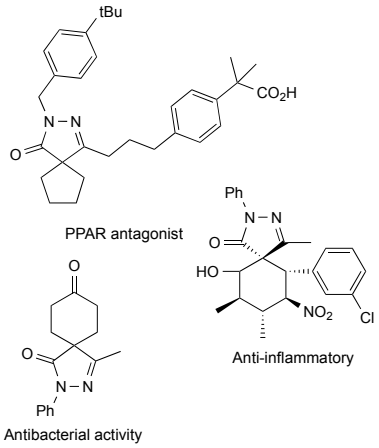

Fig 1 Some representative biologically active spiropyrazolones with a quaternary centre in C4 position.

However, to the best of our knowledge there are no examples describing the preparation of spiropyrazolone γ-butyrolactones despite the interest of this cyclic ester unit as a chiral building block for the synthesis of diverse biological active compounds and complex molecules. Instead, various organometallic[10] and organocatalytic[11] approaches have been described for the synthesis of spirooxindole γ-lactones using isatins, 3-hydroxy or methylene oxindoles as starting materials. Among them, chiral *N*-heterocyclic carbene (NHC) catalysed asymmetric reactions[12] constitute an excellent tool to synthesize these spiro

[a] GIR-SintACat-Instituto Universitario CINQUIMA y Departamento de Química Orgánica, Facultad de Ciencias, Universidad de Valladolid, Paseo Belén 7, 47011-Valladolid, Spain. E-mail: amaestro@qo.uva.es; jmandres@qo.uva.es
[b] Departamento de Química Física, University of Salamanca, 37008, Salamanca, Spain.

† Electronic Supplementary Information (ESI) available. CCDC 2110499. See DOI: 10.1039/x0xx00000x

compounds through either NHC-catalysed oxidative [3+2] annulation reaction of dioxindoles and enals,[13] the HOBt-assisted [3+2] annulation of carboxylic esters with isatins via acyl azolium intermediate,[14] or the enantioselective addition of homoenolate derived enals to isatins by cooperative NHC/Lewis acid catalysis.[15] After reviewing the existing literature, we found only three examples that describe the NHC-catalysed asymmetric synthesis of spirocyclic pyrazolones. The Biju and Yang/Zhong groups have reported the preparation of pyrazolone-fused spirocyclohexanones through [3+3] or [4+2] annulation reactions of enals or γ-chloroenals, respectively, and α-arylidene pyrazolinones (Scheme 1a and 1b).[16] On the other hand, Enders group has developed a one-pot three-component diastereo and enantioselective synthesis of spirocyclopentane pyrazolones by means of an aldol condensation followed by NHC-catalysed [3+2] annulation reaction (Scheme 1c).[17]

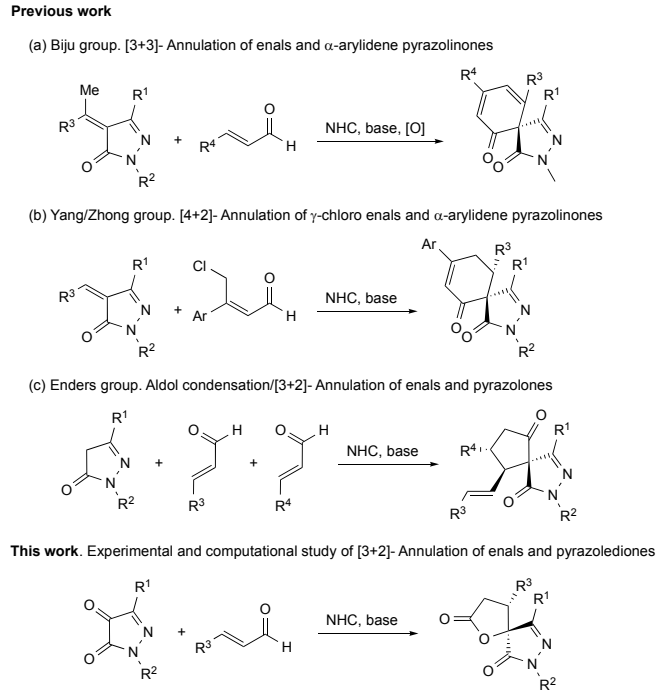

Scheme 1 Asymmetric NHC-catalysed reactions for the synthesis of spiropyrazolones.

Due to the interest of this type of compounds, herein we report their stereoselective synthesis by means a [3+2] annulation of enals and 1*H*-pyrazol-4,5-diones performed with chiral NHCs. To elucidate the mechanism of this cycloaddition reaction, we carried out electronic structure calculations at a density functional theory (DFT) level. These calculations also shed light on the origin of the stereoselectivity experimentally obtained.

Results and Discussion

We started our studies by combining pyrazolin-4,5-dione **1a** and cinnamaldehyde **2a** in the presence of different NHC pre-catalysts **A–E**, DABCO as base, and toluene as solvent at room temperature (Table 1). The diastereoselectivity for the reaction was excellent in almost all cases, and the spiro γ-butyrolactone **3a** was obtained as a single diastereomer (entries 1, 3–5 and 7).

The best enantiomeric ratio (86:14) and yield (72%) was achieved when *N*-mesityl triazolium salt **B** (Bode's catalyst) was used (entry 3).

Table 1 Optimization of reaction conditions.[a]

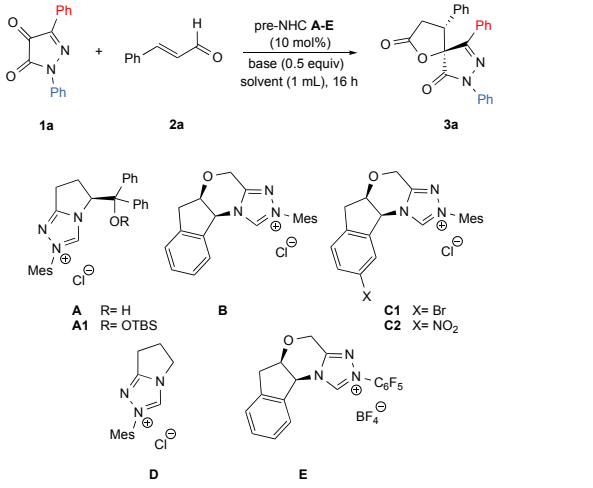

Entry	pre-NHC	Base	Solvent	Yield (%)[b]	dr[c]	er[d]
1	A	DABCO	Toluene	41	>99:<1	37:63
2	A1	DABCO	Toluene	n.r.	–	–
3	B	DABCO	Toluene	72	>99:<1	86:14
4	C1	DABCO	Toluene	38	>99:<1	79:21
5	C2	DABCO	Toluene	45	>99:<1	86:14
6	D	DABCO	Toluene	<10	n.d.	n.d.
7	E	DABCO	Toluene	31	>99:<1	50:50
8	B	DABCO	Mesitylene	65	>99:<1	87:13
9	B	DABCO	Et_2O	66	>99:<1	71:29
10	B	DABCO	THF	34	>99:<1	74:26
11	B	DABCO	DCM	50	>99:<1	77:23
12	B	DABCO	$CHCl_3$	35	>99:<1	74:26
13	B	DMAP	Toluene	62	>99:<1	79:21
14	B	TBD	Toluene	25	>99:<1	82:18
15	B	Cs_2CO_3	Toluene	8	>99:<1	87:13
16	B	DBU	Toluene	n.r.	–	–
17	B	DIPEA	Toluene	52	>99:<1	84:16
18	B	KO*t*-Bu	Toluene	29	>99:<1	88:12
19	B	NaOAc	Toluene	73	>99:<1	74:26
20	B	TMEDA	Toluene	23	>99:<1	82:18
21[e]	B	DABCO	Toluene	22	>99:<1	86:14
22[f]	B	DABCO	Toluene	62	>99:<1	79:21
23[g]	B	DABCO	Toluene	45	>99:<1	78:22
24[h]	B	DABCO	Toluene	58	>99:<1	80:20
25[i]	B	DABCO	Toluene	39	>99:<1	76:24

[a] Reaction conditions: **1a** (0.06 mmol), **2a** (0.06 mmol), pre-NHC (10 mol%), base (0.5 equiv), solvent (1 mL), at rt for 16 h. [b] Yield of **3a** after column chromatography. [c] Dr values determined by ^{1}H NMR. [d] Er values determined via chiral HPLC analysis. [e] Molar ratio **1a**:**2a** 1:2. [f] Molar ratio **1a**:**2a** 1.2:1. [g] LiCl as additive. [h] 0°C. [i] 7 mol% of catalyst **B**.

Journal Name ARTICLE

View Article Online
DOI: 10.1039/D1QO01462E

When a strong electron-withdrawing group was introduced on the indanol ring (catalyst **C2**) no change in the enantioselectivity was produced but the yield decreased dramatically (entry 5). A total loss of enantio-discrimination was observed when catalyst **E** with a pentafluorophenyl group was used (entry 7). Unfortunately, no [3+2] annulation was observed when using pre-catalyst **A1** derived from (*S*)-pyroglutamic acid with a silyl ether substituent (entry 2).[18] Achiral catalyst **E** afforded racemic adduct **3a** with low yield (entry 6). With Bode's catalyst as the most suitable among those examined, solvent screening indicated that toluene was the best solvent for this reaction because although mesitylene kept the same level of enantioselectivity (87:13, entry 8), the yield was slightly lower. Further optimization was carried out to found the best base to access the *N*-heterocyclic carbene catalyst (entries 13–20). Although the reaction works well with different bases, DABCO was retained as the base of choice. Inorganic bases as Cs_2CO_3 or KO*t*-Bu gave the desired product with high diastereo- and enantioselectivity, although with lower yield. On the other hand, in the reactions promoted with bases such as DMAP or NaOAc the enantioselectivity decreased slightly. When DBU was used as the base, no reaction was observed. Finally, other parameters were evaluated (entries 21–25). However, neither the pyrazolin-4,5-dione/enal molar ratio, nor the presence of additives nor the temperature led to an improvement of the previous er and yields.

The scope of the reaction was first examined by modification of the substituents of pyrazolin-4,5-dione. The diastereoselectivity remained excellent (>99:<1) except in the case of substrates having a non-bulky alkyl substituent (R^1), such as a methyl group (**3b**) (Table 2, entry 2).

Table 2 Substrate scope for pyrazolin-4,5-diones **1a–f**.[a]

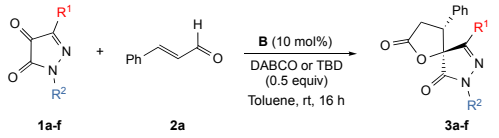

1a-f **2a** **3a-f**

Entry	R^1, R^2	Base	Yield (%)[b]	dr[c]	er[d]
1	Ph, Ph, **3a**	DABCO	72	>99:<1	86:14
2	Me, Ph, **3b**	DABCO	49	77:23	81:19[e]
3	*t*-Bu, Ph, **3c**	DABCO	73	>99:<1	73:27
4	*t*-Bu, Ph, **3c**	TBD	63	>99:<1	87:13
5	Naph, Ph, **3d**	DABCO	45	>99:<1	81:19
6	Ph, Me, **3e**	DABCO	65	>99:<1	80:20
7	*t*-Bu, Me, **3f**	TBD	58	>99:<1	84:16

[a] Reaction conditions: **1a–f** (0.06 mmol), **2a** (0.06 mmol), **B** (10 mol%), DABCO or TBD (0.5 equiv), toluene (1 mL), at rt for 16 h. [b] Yield of **3** after column chromatography. [c] Dr values determined by ^{1}H NMR. [d] Er values determined via chiral HPLC analysis. [e] Er for major diastereomer.

It should be noted that a base change is necessary to maintain the level of enantioselectivity in case of 3-*tert*-butyl substituted pyrazolin-4,5-diones. In this case, 1,5,7-triazabicyclo[4.4.0]dec-5-ene (TBD) (entries 3, 4 and 7) was the most suitable base leading to **3c** and **3f** with total diastereoselectivity and good enantioselectivity (see Supporting Information for optimization of reaction conditions, table S2).

Next, we studied the influence of the enal by using aliphatic and aromatic α,β-unsaturated aldehydes (Table 3). The reaction of pyrazolin-4,5-dione **1a** with *para*-halo substituted cinnamaldehydes worked well, furnishing the desired spiro compounds **3ab** and **3ac** in good yields with total diastereoselectivity and good enantioselectivity. As can be seen, the presence of strongly electron-withdrawing (NO_2) and electron-donating (MeO) groups in this position of enal led to the lactones **3ad** and **3ae** in good yields but with lower enantioselectivity. However, C-3 *tert*-butyl substituted pyrazolin-4,5-dione **3c** reacted with different *p*-substituted cinnamaldehydes affording adducts **3cb–3ce** with better enantiomeric ratios independently of the electronic properties of the substituent present in the aromatic ring. The introduction of a methoxy group at the *ortho*-position of the aryl ring resulted in a significant decrease in both yield and enantioselectivity (**3cf**). The reaction also tolerates an *N*-methyl group to provide, in a diastereoselective way, the desired product **3fb** in 71% yield with a good er of 90:10. Interestingly, the reaction also works with enals bearing a β-methyl substituent giving the corresponding products (**3ag** and **3cg**) with good yields, very high diastereoselectivity (>99:<1), and moderate to good enantioselectivities (er 80:20–92:8).

Table 3 Substrate scope for enals **2b–g**.[a]

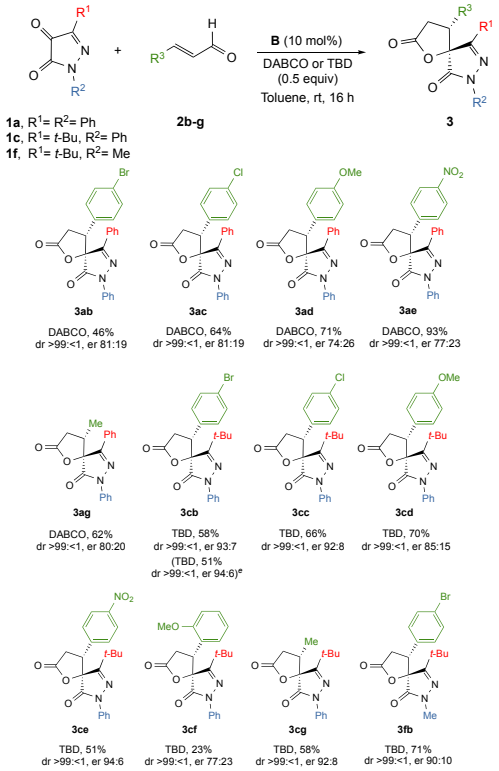

[a] Reaction conditions: **1** (0.06 mmol), **2b–g** (0.06 mmol), **B** (10 mol%), DABCO or TBD (0.5 equiv), toluene (1 mL), at rt for 16 h. [b] Yield of **3** after column chromatography. [c] Dr values determined by ^{1}H NMR. [d] Er values determined via chiral HPLC analysis. [e] **1c** (1.3 mmol), **2b** (1.3 mmol), TBD (0.5 equiv), toluene (15 mL), at rt for 16 h.

View Article Online
DOI: 10.1039/D1QO01462E

To demonstrate the synthetic utility of this reaction, a gram-scale synthesis of spiro compound **3cb** was carried out. Although it was observed a slight decrease in the yield, both diastereoselectivity and enantioselectivity remained excellent (Table 3, entry **3cb**).

In order to determinate the absolute configuration of products, optically pure (4*R*,5*S*)-4-(4-chlorophenyl)-7,9-diphenyl-1-oxa-7,8-diazaspiro[4.4]non-8-ene-2,6-dione, (−)-**3ac** was isolated after recrystallization from chloroform.[19] X-ray crystallographic analysis of a single-crystal confirmed the absolute configuration as (4*R*,5*S*) for the spirocycle (see the Supporting Information for details).

Computational Methods and Model Reaction

To elucidate the mechanism of the NHC-catalysed [3+2] asymmetric annulation, and rationalise the origin of the enantio- and diastereoselectivity observed, we carried out electronic structure calculations. The stationary points (minima and saddle points) were optimized at the M06-2X/6-31G(d,p)[20] level of theory using Gaussian16.[21] Solvation effects were included using the SMD continuum solvation model,[22] with the default parameters for toluene.

Frequencies were calculated to ensure the convergence and intrinsic reaction coordinate (IRC) calculations were carried out to confirm that the transition states obtained connect reactants and products.[23] Subsequently, single-point calculations of the stationary points were computed at a M062X/maug-cc-pVTZ level, and the free-energies reported were obtained by adding the electronic energy at the M062X/maug-cc-pVTZ level of theory with the thermal free energies computed at the M062X/6-31G(d, p) level. This selection of functional and basis set was done according to recent benchmarks,[24] and the overall procedure is similar to those followed in the literature for the study of other NHC-catalysed [3+2] asymmetric annulations.[25]

To study the NHC-catalysed [3+2] asymmetric annulations performed in this work, we used as a model the reaction between **R2(1c)** and **R1(2e)**, (Scheme 2) for which the highest er (94:6) was experimentally obtained (see Table 3).

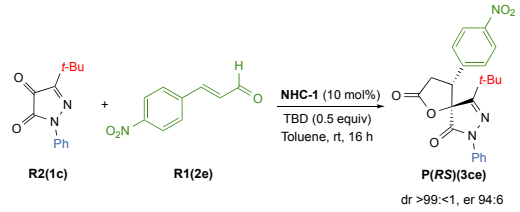

Scheme 2 NHC-catalysed [3+2] asymmetric annulation model used in the calculations.

The mechanism that emerges from our calculations is depicted in Scheme 3. In it, we can differentiate two different stages. In the first stage, the NHC catalyst reacts with the aldehyde moiety of **R1(2e)**, forming a new C-C bond, and finally leading to the **IM2**.

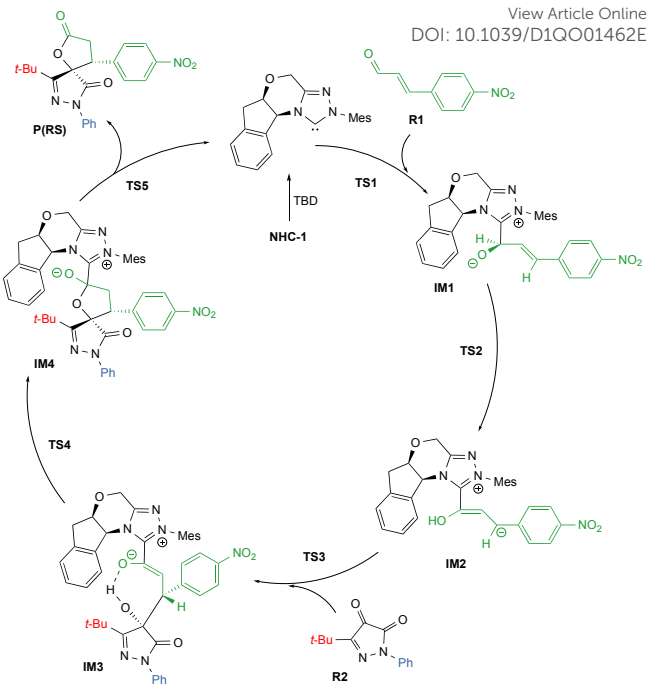

Scheme 3 Catalytic cycle of [3+2] cycloaddition reaction.

The free energy profile for the first stage is shown in Scheme 4. According to our calculations, the rate-limiting step in this stage is the hydrogen migration and formation of Breslow intermediate. The free energy barrier for the intramolecular hydrogen migration is too high (> 50 kcal/mol). However, this energy barrier shrinks to 27.56 kcal/mol if assisted by two water molecules that could be present in catalytic concentrations in the bulk, and to 22.92 kcal/mol if hydrogen migration is assisted by TBD.[26] Depending on the side of the carbene attack with respect to the aldehyde, the reaction can proceed via a *Re*/*Si* path. As it is shown in Scheme 4, the barrier for the *Si* mechanism is larger, regardless of whether the reaction is assisted by water or TBD. Accordingly, from this step, we only focused on the *Re* mechanism.

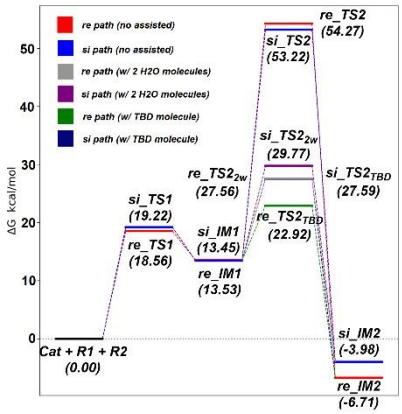

Scheme 4 Free-energy profile of the first stage of the reaction. The solvation-corrected relative free-energies at the SMD(toluene)/M06-2X/maug-cc-pVTZ level are given in kcal/mol. Cartesian coordinates of all the stationary points are shown in the Supporting Information.

In the second stage, whose free-energy profile is depicted in Scheme 5, **R2(1c)** reacts with the activated aldehyde (***Re*_IM2**), leading to the formation of **P(3ce)** and the release of the NHC

View Article Online
DOI: 10.1039/D1QO01462E

catalyst. This stage consists of three further steps, addition of the pyrazolin-4,5-dione (3rd step), formation of the lactone (4th step), and release of NHC (5th step). Of these steps, the 4th step is the rate-limiting step and also will determine the er and dr ratios. In our calculations, the 4th step is divided in two stages. In a first stage, the basis assists the proton transfer from a hydroxyl group at C4-position of the pyrazoldione moiety to the α-carbon atom of the homoenolate intermediate, a process that is associated with high energy barriers. Then the dissociation of TBD occurs and spontaneous rearrangement to **IM4**.

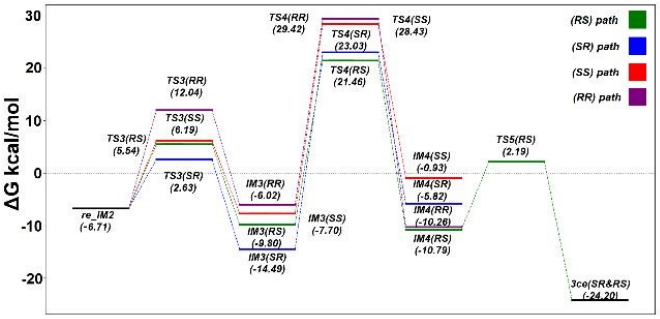

Scheme 5 Free-energy profile of the second stage of the reaction. The solvation-corrected relative free-energies at the SMD(toluene)/M06-2X/maug-cc-pVTZ level are given in kcal/mol. Cartesian coordinates of all the stationary points are shown in the Supporting Information.

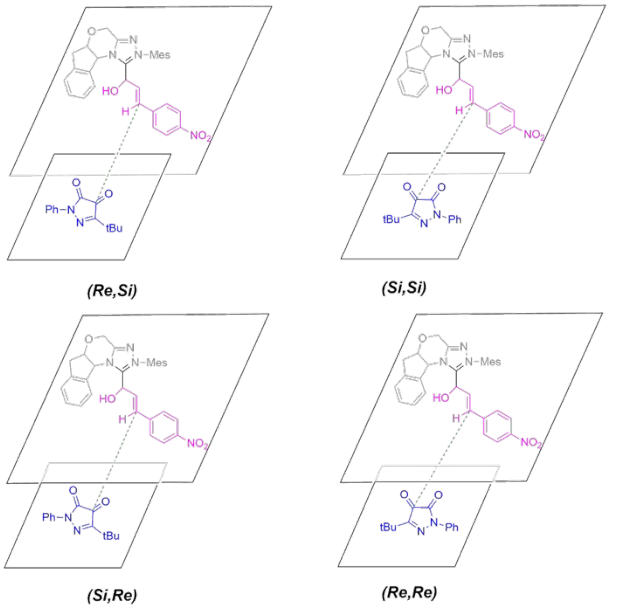

Fig 2 Diagram of the four possible modes of attack of **R2(1c)** on ***Re*_IM2**. The coordinates of the transition states originated from these modes of attack are shown in the Supporting Information, and their energies are depicted in Scheme 5 (**TS3**).

As it is depicted in Figure 2, depending on the attack mode of the pyrazoldione **R2(1c)** in the 3rd step, and as a consequence of the presence of two prochiral faces in both **R2** as Breslow intermediate ***Re*_IM2**, we could find four different mechanisms that will produce four different stereoisomers (*SS*), (*SR*), (*RR*) and (*RS*). The formation of rotational conformers associated with the *Z*-configuration of the C=C bond was not feasible due to the high energy barrier associated with C=C torsion (above 30 kcal/mol). Although the free-energy barrier for the four pathways is considerably different ranging from 2.63 to 12.04 kcal/mol, all barriers are well below those obtained in the 4th step. In this step, formation of the lactone proceeds via protonation of the basis (TBD). Our calculations predict that the free energy barrier is lower for the (*RS*) mechanism, which after NHC release that proceeds with almost no barrier, will produce the **P(*RS*)(3ce)** product. This is also the main product obtained experimentally (with an er of 94:6).

To rationalize the origin of the enantioselectivity, we analyse the structure of the four **TS4** (shown in Scheme S6 in the Supporting Information). According to **TS4** structures, there is a good correlation between the degree of synchronicity of the two proton transfer steps at the saddle point and the energy barrier, as it was previously observed for Diels-Alder reactions.[27] For the **TS4**(*SR*) and **TS4**(*RS*) structures, both protons are located between **IM3** and TBD at the TS, while for **TS4**(*SS*) the OH group of pyrazoldione has not been deprotonated, and for **TS4**(*RR*) this proton has already been transferred to TBD. To quantify the origin of the differences, we combine the distortion-interaction analysis (following the analysis carried out for other NHC-catalysis articles[25a,d,28]) with the energy decomposition analysis (carried out using QChem 5.2[29,30]) and a 6-31G basis set. Leaving aside the entropic contribution, stabilization of the **TS4**(*RS*) is traced back from a more favourable interaction, which is induced by the relaxation of the molecular orbitals of the fragments (lower polarization energy. For details see Scheme S7 and Tables S3 and S4 in the Supporting Information).

Conclusions

In the present work, we have described the first asymmetric synthesis of spiropyrazolone γ-butyrolactones from 1*H*-pyrazol-4,5-diones and enals by an NHC-catalysed [3+2] annulation process. The developed protocol is mild and tolerates a wide range of substituents on both substrates. The use of Bode's catalyst in this cascade reaction provided the enantioenriched spirocyclic compounds containing two contiguous stereogenic centres in good yields with excellent diastereoselectivity and

good enantioselectivity. To understand the catalytic mechanism and origin of stereoselectivity, electronic structure calculations were carried out. These indicate that the Brønsted base used to generate the carbene NHC, also assists the hydrogen migration for the generation of homoenolate. Furthermore, the formation of the lactone that proceeds after the pyrazolin-4,5-dione attack on the Breslow intermediate is the rate-limiting step and determining of the enantio- and diastereomeric ratios. The pathway responsible for the *RS*-configuration of spirocyclic pyrazolones has been identified to be the most favourable one.

Author Contributions

Conceptualization and methodology, A. M. and J. M. A. Investigation and writing-original draft, A. M., M. G. O and P. G. J. Electronic structure calculations, P. O. and P. G. J. Writing-review & editing, A. M. and J. M. A. Funding acquisition, J. M. A.

Conflicts of interest

There are no conflicts to declare.

Acknowledgements

A. M. and J. M. A. thank Junta de Castilla y León (Projects: FEDER-VA115P17, and VA149G18) for financial support and the Laboratory of Instrumental Techniques (LTI) Research Facilities, Universidad de Valladolid. M. G. O. also thanks Junta de Castilla y León for a predoctoral fellowship (EDU/556/2019). The aid in the X-Ray diffraction determination provided by Ignacio Pérez Ortega is also acknowledged. P. O. and P. G. J. gratefully acknowledged grant PID2020-113147GA-I00 funded by MCIN/AEI/10.13039 and by the Fundación Salamanca City of Culture and Knowledge (programme for attracting scientific talent to Salamanca). P. O. acknowledges Grant No. EDU/601/2020 (Junta de Castilla y Leon and European Social Fund).

Notes and references

1 *(a)* P. K. Mykhailiuk, Fluorinated Pyrazoles: From Synthesis to Applications, *Chem. Rev*., 2021, **121**, 1670; *(b)* A. Schmidt and A. Dreger, Recent Advances in the Chemistry of Pyrazoles. Properties, Biological Activities, and Syntheses, *Curr. Org. Chem.*, 2011, **15**, 1423; *(c)* S. Fustero, M. Sánchez-Roselló, P. Barrio and A. Simón-Fuentes, From 2000 to Mid-2010: A Fruitful Decade for the Synthesis of Pyrazoles, *Chem. Rev.*, 2011, **111**, 6984.

2 *(a)* A. Szukalski, B. Sahraoui, B. Kulyk, C. A. Lazar, A. M. Manea and J. Mysliwiec, Chemical Structure versus Second-Order Nonlinear Optical Response of the Push–Pull Type Pyrazoline Based Chromophores, *RSC Adv.,* 2017, **7***,* 9941; *(b)* C. Ye, G. L. Gard, R. W. Winter, R. G. Syvret, B. Twamley and J. M. Shreeve, Synthesis of Pentafluorosulfanylpyrazole and Pentafluorosulfanyl-1,2,3-triazole and Their Derivatives as Energetic Materials by Click Chemistry, *Org. Lett*., 2007, **9**, 3841; *(c)* K. Dedeian, J. Shi, N. Shepherd, E. Forsythe and D. C. Morton, Photophysical and Electrochemical Properties of Heteroleptic Tris-Cyclometalated Iridium (III) Complexes, *Inorg. Chem.,* 2005, **44***,* 4445.

3 (*a)* T. -F. Wang, S. R. Kosuru, S. -C. Yu, Y. -C. Chang, H. -Y. Lai, Y. -L. Chang, K. -H. Wu, S. Dingad and H. -Y. Chen, Use of Pyrazoles as Ligands Greatly Enhances the Catalytic Activity of Titanium Iso-Propoxide for the Ring-Opening Polymerization of L-Lactide: a Cooperation Effect, *RSC Adv.,* 2020, **10**, 40690; *(b)* S. O. Ojwach and J. Darkwa, Pyrazole and (Pyrazol-1-yl)metal Complexes as Carbon–Carbon Coupling Catalysts, *Inorg. Chim. Acta,* 2010, **363**, 1947; *(c)* R. A. Singer, M. Doré, J. E. Sieser and M. A. Berliner, Development of Nonproprietary Phosphine Ligands for the Pd-Catalyzed Amination Reaction, *Tetrahedron Lett.,* 2006, **47**, 3727.

4 *(a)* S. R. Mandha, S. Siliveri, M. Alla, V. R. Bommena, M. R.; Bommineni and B. Balasubramanian, Eco-Friendly Synthesis and Biological Evaluation of Substituted Pyrano[2,3-C]Pyrazoles, Bioorg. Med. *Chem. Lett.*, 2012, **22**, 5272; *(b)* ''Dipyrone''. Martindale: The Complete Drug Reference, ed. A. Brayfield, Pharmaceutical Press, 2014; *(c)* G. Varvounis, 2 Pyrazol-3-ones. Part IV: Synthesis and Applications, *Adv. Heterocycl. Chem.*, 2009, **98**, 143; *(d)* W. Ji Yuan, T. Yasuhara, T. Shingo, K. Muraoka, T. Agari, M. Kameda, T. Uozumi, N. Tajiri, T. Morimoto, M. Jing, T. Baba, F. Wang, H. Leung, T. Matsui, Y. Miyoshi and I. Date, Neuroprotective Effects of Edaravone-Administration on 6-OHDA-Treated Dopaminergic Neurons, *BMC Neurosci.*, 2008, **9**, 75; *(e)* H. Yoshida, H. Yanai, Y. Namiki, K. Fukatsu-Sasaki, N. Furutani and N. Tada, Neuroprotective Effects of Edaravone: a Novel Free Radical Scavenger in Cerebrovascular Injury, *CNS Drug Rev*., 2006, **12**, 9; *(f)* T. Watanabe, K. Tanaka, K. Watanabe, Y. Takamatsu and A. Tobe, Research and Development of the Free Radical Scavenger Edaravone as a Neuroprotectant, *Yakugaku Zasshi*, 2004, **124**, 99.

5 *(a)* N. S. Stock, A. C. -Y. Chen, Y. M. Bravo, J. D. Jacintho and Y. Truong, US 20180079745A1, 2018; *(b)* Y. Zhang, S. Wu, S. Wang, K. Fang, G. Dong, N. Liu, Z. Miao, J. Yao, J. Li, W. Zhang, C. Sheng and W. Wang, Divergent Cascade Construction of Skeletally Diverse "Privileged" Pyrazole-Derived Molecular Architectures, *Eur. J. Org. Chem*., 2015, 2030; *(c)* B. Han, S. Xu and P. Wang, CN Patent CN104610148, 2015; *(d)* P. S. Silaychev, V. O. Filimonov, A. N. Maslivets and R. R. Makhmudov, Patent, RU2577528, 2014; *(e)* M. S. Chande, P. A. Barve and V. Suryanarayan, Synthesis and Antimicrobial Activity of Novel Spirocompounds with Pyrazolone and Pyrazolthione Moiety, *J. Heterocycl. Chem.*, 2007, **44**, 49.

6 *(a)* L. Carceller-Ferrer, G. Blay, J. R. Pedro and C. Vila, Recent Advances in Catalytic Enantioselective Synthesis of Pyrazolones with a Tetrasubstituted Stereogenic Center at the 4-Position, *Synthesis*, 2021, **53**, 215; *(b)* X. Xie, L. Xiang, C. Peng and B. Han, Catalytic Asymmetric Synthesis of Spiropyrazolones and their Application in Medicinal Chemistry, *Chem. Rec.*, 2019, **19**, 2209; *(c)* S. Liu, X. Bao and B. Wang, Pyrazolone: A Powerful Synthon for Asymmetric Diverse Derivatizations, *Chem. Commun.*, 2018, **54**, 11515.

7 For reviews, see: *(a)* Y. Yang, X. Wang, X. Ye, B. Wang, X. Bao and H. Wang, Advances of α-Activated Cyclic Isothiocyanate for the Enantioselective Construction of Spirocycles, *Org. Biomol. Chem.*, 2021, **19**, 4610. For selected examples, see: *(b)* W. Wang, X. Bao, S. Wei, S. Nawaz, J. Qu and B. Wang, Asymmetric Sequential Annulation/Aldol Process of 4-Isothiocyanato Pyrazolones and Allenones: Access to Novel Spiro[Pyrrole–Pyrazolones] and Spiro[Thiopyranopyrrole–Pyrazolones], *Chem. Commun.*, 2021, **57**, 363; *(c)* W. Wang, S. Wei, X. Bao, S. Nawaz, J. Qu and B. Wang, Enantioselective [3 + 2] Annulation of 4-Isothiocyanato Pyrazolones and Alkynyl Ketones Under Organocatalysis, *Org. Biomol. Chem.*, 2021, **19**, 1145; *(d)* X. Bao, S. Wei, X. Qian, J. Qu, B. Wang, L. Zou and G. Ge, Enantioselective Construction of Dispirotriheterocycles

DOI: 10.1039/D1QO01462E

Featuring a 4-Aminopyrazolone Motif Through a Cascade Michael/Cyclization Process, *Chem. Commun.*, 2020, **56**, 10690; *(e)* X. Bao, S. Wei, X. Qian, J. Qu, B. Wang, L. Zou and G. Ge, Asymmetric Construction of a Multi-Pharmacophore-Containing Dispirotriheterocyclic Scaffold and Identification of a Human Carboxylesterase 1 Inhibitor, *Org. Lett.*, 2018, **20**, 3394.

8 S. Meninno, A. Roselli, A. Capobianco, J. Overgaard and A. Lattanzi, Diastereodivergent and Enantioselective Access to Spiroepoxides via Organocatalytic Epoxidation of Unsaturated Pyrazolones, *Org. Lett.*, 2017, **19**, 5030.

9 *(a)* M. -M. Chu, S. -S. Qi, Y. -F. Wang, B. Wang, Z. -H. Jiang, D. -Q. Xu and Z. -Y. Xu, Organocatalytic Asymmetric [4 + 1] Annulation of in Situ Generated Ortho-Quinomethanes with 4-Halo Pyrazolones: Straightforward Access to Chiral Spiro-Benzofuran Pyrazolones, *Org. Chem. Front.*, 2019, **6**, 1977; *(b)* J. Zhou, W. -J. Huang and G. -F. Jiang, Synthesis of Chiral Pyrazolone and Spiropyrazolone Derivatives through Squaramide-Catalyzed Reaction of Pyrazolin-5-ones with o-Quinone Methides, *Org. Lett.*, 2018, **20**, 1158.

10 B. M. Trost and K. Hirano, Dinuclear Zinc Catalyzed Asymmetric Spirannulation Reaction: An Umpolung Strategy for Formation of α-Alkylated-α-Hydroxyoxindoles, *Org. Lett.*, 2012, **14**, 2446.

11 *(a)* Z. -T. Yang, J. Zhao, W. -L. Yang and W. -P. Deng, Enantioselective Construction of CF_3-Containing Spirooxindole γ-Lactones via Organocatalytic Asymmetric Michael/Lactonization, *Org. Lett.*, 2019, **21**, 1015; *(b)* L. Chen, Z. -J. Wu, M. -L. Zhang, D. -F. Yue, X. -M. Zhang, X. -Y. Xu and W. -C. Yuan, Organocatalytic Asymmetric Michael/Cyclization Cascade Reactions of 3-Hydroxyoxindoles/3-Aminooxindoles with α,β-Unsaturated Acyl Phosphonates for the Construction of Spirocyclic Oxindole-γ-lactones/lactams, *J. Org. Chem.*, 2015, **80**, 12668; *(c)* S. Jayakumar, S. Muthusamy, M. Prakash and V. Kesavan, Enantioselective Synthesis of Spirooxindole α-exo-Methylene-γ-butyrolactones from 3-OBoc-Oxindoles, *Eur. J. Org. Chem.*, 2014, 1893; *(d)* Q. -L. Wang, L. Peng, F. -Y. Wang, M. -L. Zhang, L. -N. Jia, F. Tian, X. -Y. Xu and L. -X. Wang, An Organocatalytic Asymmetric Sequential Allylic Alkylation–Cyclization of Morita–Baylis–Hillman Carbonates and 3-Hydroxyoxindoles, *Chem. Commun.*, 2013, **49**, 9422.

12 For reviews on cascade reactions, see: *(a)* C. Zhao, S. A. Blaszczyk and J. Wang, Asymmetric reactions of N-Heterocyclic Carbene (NHC)-Based Chiral Acyl Azoliums and Azolium Enolates, *Green Synthesis and Catalysis* 2021, **2**, 198. *(b)* S. Mondal, S. R. Yetra, S. Mukherjee and A. T. Biju, NHC-Catalyzed Generation of α,β-Unsaturated Acylazoliums for the Enantioselective Synthesis of Heterocycles and Carbocycles, *Acc. Chem. Res.* 2019, **52**, 425. *(c)* X. -Y. Chen, S. Li, F. Vetica, M. Kumar and D. Enders, N-Heterocyclic-Carbene-Catalyzed Domino Reactions via Two or More Activation Modes, *iScience* 2018, **2**, 1. *(d)* E. Reyes, U. Uria, L. Carrillo and J. L. Vicario, Enantioselective Cascade Reactions under N-Heterocyclic Carbene Catalysis, *Synthesis* 2017, **49**, 451. *(e)* C. Zhang, J. F. Hooper and D. W. Lupton, N-Heterocyclic Carbene Catalysis via the α,β-Unsaturated Acyl Azolium, *ACS Catal.* 2017, **7**, 2583.

13 X. -Y. Chen, K. -Q. Chen, D. -Q. Sun and S. Ye, N-Heterocyclic Carbene-Catalyzed Oxidative [3 + 2] Annulation of Dioxindoles and Enals: Cross Coupling of Homoenolate and Enolate, *Chem. Sci.*, 2017, **8**, 1936.

14 J. Xu, S. Yuan, M. Miao and Z. Chen, 1-Hydroxybenzotriazole-Assisted, N-Heterocyclic Carbene Catalyzed β-Functionalization of Saturated Carboxylic Esters: Access to Spirooxindole Lactones, *J. Org. Chem.*, 2016, **81**, 11454.

15 J. Dugal-Tessier, E. A. O'Bryan, T. B. H. Schroeder, D. T. Cohen and K. A. Scheidt, An N-Heterocyclic Carbene/Lewis Acid Strategy for the Stereoselective Synthesis of Spirooxindole Lactones, *Angew. Chem. Int. Ed.*, 2012, **51**, 4963.

16 *(a)* C. Zhao, K. Shi, G. He, Q. Gu, Z. Ru, L. Yang and G. Zhong, NHC-Catalyzed Asymmetric Formal [4+2] Annulation to Construct Spirocyclohexane Pyrazolone Skeletons, *Org. Lett.*, 2019, **21**, 7943; *(b)* S. Reddy Yetra, S. Mondal, S. Mukherjee, R. G. Gonnade and A. T. Biju, Enantioselective Synthesis of Spirocyclohexadienones by NHC Catalyzed Formal [3+3] Annulation Reaction of Enals, *Angew. Chem. Int. Ed.*, 2016, **55**, 268.

17 L. Wang, S. Li, P. Chauhan, D. Hack, A. R. Philipps, R. Puttreddy, K. Rissanen, G. Raabe and D. Enders, Asymmetric, Three-Component, One-Pot Synthesis of Spiropyrazolones and 2,5-Chromenediones from Aldol Condensation/NHC-Catalyzed Annulation Reactions, *Chem. Eur. J.*, 2016, **22**, 5123.

18 *(a)* X. -Y. Chen, Z. -H. Gao and S. Ye, Bifunctional N-Heterocyclic Carbenes Derived from L-Pyroglutamic Acid and Their Applications in Enantioselective Organocatalysis, *Acc. Chem. Res.*, 2020, **53**, 690; *(b)* L. -H. Sun, L. -T. Shen and S. Ye, Highly Diastereo- and Enantioselective NHC-Catalyzed [3+2] Annulation of Enals and Isatins, *Chem. Commun.*, 2011, **47**, 10136.

19 Er >99: <1 was confirmed via chiral HPLC analysis. CCDC 2110499 (**3ac**) contains the supplementary crystallographic data for this paper.

20 Y. Zhao and D. G. Truhlar, The M06 Suite of Density Functionals for Main Group Thermochemistry, Thermochemical Kinetics, Noncovalent Interactions, Excited States, and Transition Elements: Two New Functionals and Systematic Testing of Four M06-Class Functionals and 12 other Functionals, *Theor. Chem. Acc.*, 2008, **120**, 215.

21 M. J. Frisch, G. W. Trucks, H. B. Schlegel, G. E. Scuseria, M. A. Robb, J. R. Cheeseman et al., Gaussian-16 Revision A.03 (Gaussian Inc., Wallingford CT, 2016).

22 A. V. Marenich, C. J. Cramer and D. G. Truhlar, Universal Solvation Model Based on Solute Electron Density and on a Continuum Model of the Solvent Defined by the Bulk Dielectric Constant and Atomic Surface Tensions, *J. Phys. Chem. B*, 2009, **113**, 6378.

23 A. Hollwarth, M. Bohme, S. Dapprich, A. W. Ehlers, A. Gobbi, V. Jonas, K. F. Kohler, R. Stegmann, A. Veldkamp and G. Frenking, A Set of d-Polarization Functions for Pseudo-Potential Basis Sets of the Main Group Elements Al-B1 and f-Type Polarization Functions for Zn, Cd, Hg, *Chem. Phys. Lett.*, 1993, **208**, 237.

24 *(a)* E. Papajak and D. G. Truhlar, Convergent Partially Augmented Basis Sets for Post-Hartree−Fock Calculations of Molecular Properties and Reaction Barrier Heights, *J. Chem. Theory Comput.*, 2010, **6**, 597; *(b)* S. Rayne and K. Forest, A Comparative Examination of Density Functional Performance Against the ISOL24/11 Isomerization Energy Benchmark, *J. Comp. Theor. Chem.*, 2016, **1090**, 147.

25 *(a)* Y. Li, Z. Li and Z. Zhang, A Computational Study on NHC-Catalyzed [3+4] Annulation between Isatin-Derived Enal and Aurone-Derived Azadiene: Insights into Mechanism and Stereoselectivity, *Molecular Catalysis*, 2020, **496**, 111183; *(b)* Y. Li and Z. Zhang, Mechanisms and Stereoselectivities of NHC-Catalyzed [3+4] Cycloaddition Reaction between Isatin-Derived Enal and *N*-(ortho-Chloromethyl)aryl Amide, *Eur. J. Org. Chem.*, 2019, 2989; *(c)* J. Gao and Y. Wang, Mechanistic Studies on the *N*-Heterocyclic Carbene-Catalyzed Reaction of Isatin-Derived Enals with Hydrazones, *Org. Biomol. Chem.*, 2019, **17**, 7442; *(d)* Y. Li, Z. Zhang and C. Liang, Understanding the Mechanism and Stereoselectivity of NHC-Catalyzed [3+2] Cycloaddition of 3-Bromoenals and Isatin *N*-Boc Ketimines, *Org. Biomol. Chem.*, 2018, **16**, 9251; *(e)* Y. Reddi and R. B. Sunoj, Origin of Stereoselectivity in Cooperative Asymmetric Catalysis Involving *N*-Heterocyclic Carbenes and Lewis Acids

View Article Online
DOI: 10.1039/D1QO01462E

toward the Synthesis of Spirooxindole Lactone, *ACS Catal.,* 2017, **7**, 530.
26 M. J. Ajitha and C. H. Suresh, Role of Base Assisted Proton Transfer in *N*-Heterocyclic Carbene-Catalyzed Intermolecular Stetter Reaction, *Tetrahedron Lett.*, 2013, **54**, 7144.
27 P. Vermeeren, T. A. Hamlin and F. M. Bickelhaupt, Origin of Asynchronicity in Diels-Alder Reactions, *Phys. Chem. Chem. Phys.*, 2021, **23**, 20095.
28 Y. Lin and Z. Zhang, Mechanism and Stereoselectivity in NHC-Catalyzed β-Functionalization of Saturated Carboxylic Ester, *RSC Adv.*, 2019, **9**, 7635.
29 R. Z. Khaliullin, E. A. Cobar, R. C. Lochan, A. T. Bell and M. Head-Gordon, Unravelling the Origin of Intermolecular Interactions Using Absolutely Localized Molecular Orbitals, *J. Phys. Chem. A*, 2007, **111**, 8753.
30 Y. Shao, Z. Gan, E. Epifanovsky, A. T. B. Gilbert, M. Wormit, J. Kussmann, et al., Advances in Molecular Quantum Chemistry Contained in the Q-Chem 4 Program Package*, Mol. Phys*., 2015, **113**, 184.